

See discussions, stats, and author profiles for this publication at: <https://www.researchgate.net/publication/263956127>

Influence of Nanoscale Confinement on the Molecular Mobility of Ibuprofen

ARTICLE in THE JOURNAL OF PHYSICAL CHEMISTRY C · JUNE 2014

Impact Factor: 4.77 · DOI: 10.1021/jp500630m

CITATIONS

6

READS

53

6 AUTHORS, INCLUDING:



Ana Rita Brás

University of Cologne

32 PUBLICATIONS 410 CITATIONS

SEE PROFILE



A. Schönhals

Bundesanstalt für Materialforschung und -prü...

187 PUBLICATIONS 3,643 CITATIONS

SEE PROFILE

Influence of Nanoscale Confinement on the Molecular Mobility of Ibuprofen

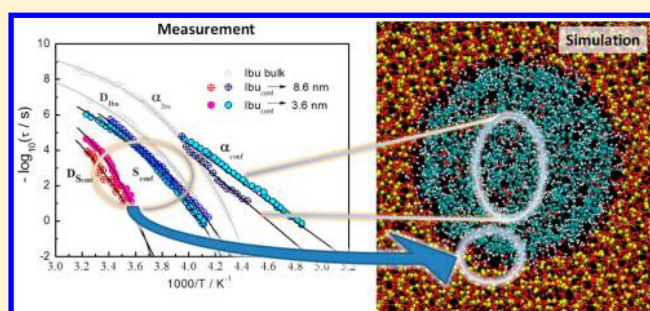
Ana R. Brás,^{†,‡} Isabel M. Fonseca,[†] Madalena Dionísio,[†] Andreas Schönhals,[‡] Frédéric Affouard,[§] and Natália T. Correia^{*,†,§}

[†]REQUIMTE, Departamento de Química, Faculdade de Ciências e Tecnologia, Universidade Nova de Lisboa, 2829-516 Caparica, Portugal

[‡]BAM Federal Institute for Materials Research and Testing, D-12205 Berlin, Germany

[§]Unité Matériaux Et Transformations (UMET), UMR CNRS 8207, UFR de Physique, BAT P5, Université Lille Nord de France, F-59655 Villeneuve d'Ascq Cedex, France

ABSTRACT: The molecular mobility of ibuprofen confined to a mesoporous silica host (MCM-41) of 3.6 nm pore diameter is investigated by dielectric relaxation spectroscopy. It is confirmed that crystallization is suppressed; therefore, depending on the temperature, the guest exists in the glassy and supercooled state inside of the pores. A detailed relaxation map is provided where multiple processes are dynamically characterized, comprised of three processes that are also found for the bulk and two additional ones. The bulk-like processes include two secondary processes, a simple thermally activated one, a γ process and a Johari–Goldstein β_{JG} process, and the one associated with the dynamic glass transition of molecules located in the pore center (α process). In confinement, all of these processes display deviations in its dynamical behavior relative to the bulk, the most dramatic one undergone by the α process, which exhibits Arrhenius-like temperature dependence upon approaching the glass transition instead of Vogel/Fulcher/Tammann/Hesse (VFTH) scaling as obeyed by the bulk. The two additional relaxations are associated with the dynamical behavior of hydrogen-bonded ibuprofen molecules lying in an interfacial layer near the pore wall, an S process for which the mobility is strongly reduced relative to the α process and a Debye-like D process for which the dynamics is closely correlated to the dynamics of the interfacial process, both exhibiting VFTH temperature dependencies. The comparison with the behavior of the same guest in the analogous host, SBA-15, with a higher pore diameter (8.6 nm) leads to the conclusion that the bulk-like mobility associated with the dynamic glass transition undergoes finite size effects being accelerated upon a decrease of the pore size with a concomitant reduction of the glass transition temperature relative to the bulk, 22 and 32 K, respectively, for the 8.6 and 3.6 nm pore diameters. The continuous decrease in the separation between the α - and β_{JG} -trace with pore size decrease allows one to conclude that confined ibuprofen is a suitable guest molecule to test the Coupling Model that predicts a transformation of the α process into a β_{JG} -mode under conditions of an extreme nanoconfinement. The overall behavior inside of pores is consistent with the existence of two distinct dynamical domains, originated by ibuprofen molecules in the core of the pore cavity and adjacent to the pore wall, from which a clear picture is given by molecular dynamics simulation.



INTRODUCTION

Nanoconfinement emerged in the past few years as a strategy to manipulate/prevent crystallization^{1–3} of guest molecules and stabilize unstable metastable forms in polymorphic pharmaceuticals because their dissolution and bioavailability are usually improved.^{4,5} In particular, when crystallization is avoided, it was found that the glass transition temperature (T_g) of the incorporated glass former can be affected when the restricted geometries have dimensions in the nanometer scale.^{6–8} The thus-obtained state can have an enhanced mobility compared with that of the bulk where the acceleration in the dynamics is rationalized as an effect of the interference of the pore dimension with the characteristic length for the dynamic glass transition. This can result in a deviation from the typical curvature of the relaxation time of the dynamic glass transition

in the activation plot (Vogel/Fulcher/Tammann/Hesse law; VFTH law) to Arrhenius dependence.⁸ However, for rather low pore sizes, the guest molecules can undergo specific interactions with the pore wall, as has been shown for systems forming hydrogen bonds between the guest molecules and the inner pore surface. In this case, the molecular mobility can slow down, and the T_g value is increased.^{8,9} Therefore, in general, the dynamics of molecules confined to nanoporous hosts is controlled by a counterbalance between confinement and surface effects.⁸ This was shown recently by some of us by means of dielectric relaxation spectroscopy (DRS) for

Received: January 19, 2014

Revised: May 24, 2014

Published: May 27, 2014

ibuprofen (chemical structure shown in Figure 1) confined to mesoporous SBA-15.¹⁰ Two families of molecules with different

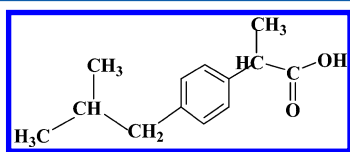


Figure 1. Chemical structure of ibuprofen ((2*RS*)-2[4-(2-methylpropyl)phenyl]propanoic acid).

molecular mobilities were observed, one due to molecules close to the pore center with a higher mobility compared to the bulk at temperatures close to T_g and another one with slower dynamics originating from molecules interacting with the pore walls. This was previously observed for ibuprofen confined to the analogue SBA mesoporous matrix by multinuclear solid-state nuclear magnetic resonance (NMR) at room temperature.¹¹

For ibuprofen impregnated in MCM-41, the confining host also in the present work, solid-state NMR measurements have shown^{3,12–14} that at room temperature, the ibuprofen molecules are extremely mobile, pointing to a liquid-like behavior of ibuprofen inside of the pores. It should be noted that ibuprofen is a crystalline solid at ambient temperature (melting temperature of $T_m = 347$ K).¹⁵ Under a nanoscale confinement, ibuprofen thus exists in a supercooled liquid state, as confirmed also by X-ray diffraction studies of ibuprofen embedded in MCM-41.¹⁶ Additionally, the NMR studies^{3,14} showed that ibuprofen molecules when confined in silica matrixes can interact through weak hydrogen bonds between the carboxylic acid group and the silanol (Si–OH) surface groups of the pores. Mesoporous silica-based materials attracted a great interest due to their particular physical properties, such as its biocompatibility, ordered pore network, high internal surface area, silanol-containing surface, as well as chemical and mechanical stability.^{17,18}

Furthermore, ibuprofen belongs to the class of hydrogen-bonded associating materials existing in the crystalline state as cyclic dimers.^{19,20} In our previous studies, the existence of intermolecular hydrogen-bonded aggregates such as dimers and trimers, either cyclic or linear, was established for supercooled liquid ibuprofen.²¹ This reflects on its complex dynamical behavior by the detection of a particular relaxation process (called the D process) at temperatures above the glass transition temperature ($T_g = 226$ K). Therefore, it is possible to evaluate the impact of a confinement on the dynamical behavior of ibuprofen, which, in bulk, exhibits multiple relaxation processes,²¹ the Debye-like D process, the main α relaxation associated with the dynamic glass transition, a β_{JG} Johari–Goldstein (JG) process taken as the precursor of the α relaxation, and a more localized secondary γ relaxation probably associated with fluctuations of carboxylic groups.

This kind of investigation can provide insights having interest under both theoretical and practical points of view. The former is related with the physics of condensed matter including glass transition phenomena, polymorphism, metastability, and the latter envisaging stabilizing forms with enhanced bioavailability and drug delivery properties.

EXPERIMENTAL SECTION

Materials. *Ibuprofen.* Racemic ibuprofen ((2*RS*)-2[4-(2-methylpropyl)phenyl]propanoic acid, C₁₃H₁₈O₂), designated hereafter as ibuprofen, was purchased from Sigma (catalogue number I4883 (CAS 15687-27-1), lot number 026H1368, 99.8% GC assay) with a molar mass of 206.28 g·mol^{−1}, and it was used without further purification; X-ray powder diffraction (XRD) characterization of the crystalline sample studied in the present work was performed by Derrolez et al.,²² confirming the crystallographic structure reported by McConnell¹⁹ and Shankland et al.²⁰ Normally, ibuprofen is a crystalline solid. However, recently, it was found that crystallization can be prevented by appropriate cooling from the melt. For details, see ref 21 and references cited there. In that case, supercooled (amorphous) ibuprofen was obtained, which is referred to as bulk amorphous ibuprofen during the course of this contribution.

MCM-41. The mesoporous MCM-41 (100% Si) matrix was synthesized and characterized according to the procedures described in a previous publication by some of us.²³ Briefly, aerosil was used as a silica source and alkyltrimethylammonium bromide as a template; calcination at a heating rate of 1 K/min to 813 K was used to completely remove the organic template. The MCM-41 matrix was kept under dry nitrogen for 1 h at 813 K followed by 6 h under dry air. Nitrogen absorption analysis was used to obtain the texture features, allowing estimation of a specific surface area of 884 m²/g and a pore diameter of 3.6 nm. This pore size is considerably smaller than the pore diameter of the previously employed SBA-15 material (8.6 nm) obtained by a corresponding procedure using copolymer templates.²³ The MCM-41 materials were routinely characterized by XRD and transmission electron microscopy (TEM). The Bragg peaks in the XRD pattern are only visible at small angles, an intense peak at $2\theta < 2^\circ$ and two weak reflection peaks between 2.5 and 3.5° being typical of the long-range ordered dimensional hexagonal mesostructure. TEM analysis confirmed the uniform honeycomb structure formed by parallel cylindrical pores organized in a hexagonal array.²³

Hereafter, MCM-41 will be called MCM.

Guest Loading. The MCM was loaded with ibuprofen as described for the SBA material elsewhere.¹⁰ Self-supported pellets of finely ground MCM powder were evacuated under vacuum (10^{−4} mbar) at 573 K for 7 h to remove water and impurities (for details, see refs 10 and 23). After this cleaning step, the pellets were cooled down to 298 K and immersed still under vacuum in a solution of ibuprofen in ethanol (~0.05 g·cm^{−3}); the pores were filled by capillary wetting followed by a solvent removal procedure by heating the sample at 333 K at normal pressure for ~12 h. Five successive impregnation steps were carried out. Between each impregnation, the solvent was removed by heating at 333 K. Finally, after one night at room temperature, the samples were carefully washed with a small amount of ethanol to remove the excess of nonconfined ibuprofen that crystallized in the outer surface of the pellet. More details on the impregnation procedure and solvent removal are given in ref 10. Samples were handled in a desiccator. The composite is called hereafter Ibu/MCM.

Experimental Techniques. *Thermogravimetry.* Thermogravimetric analysis (TGA) was used to estimate the content of ibuprofen inside of the mesoporous silica, as described previously for ibuprofen confined in comparable kind of mesoporous matrix (SBA-15).¹⁰ TGA measurements were

carried out by a Seiko TG/DTA 220 apparatus, at a heating rate of $10\text{ K}\cdot\text{min}^{-1}$ under a dry synthetic air atmosphere using a fraction of the sample prepared for the dielectric measurements. Figure 2 shows the TGA curves obtained for Ibu/MCM and

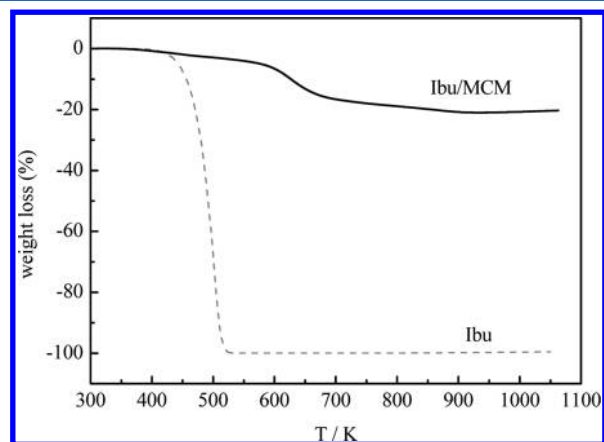


Figure 2. Thermogravimetric curves obtained upon heating at $10\text{ K}\cdot\text{min}^{-1}$ for MCM loaded with ibuprofen, Ibu/MCM, and for bulk amorphous ibuprofen, Ibu.

bulk amorphous ibuprofen. A first small step is observed until 423 K, which is related to water mass loss (1.3 wt %). The weight loss due to the burning and decomposition of the organic drug molecule is measured up to $\sim 1073\text{ K}$, allowing one to estimate a loading degree $\sim 19\text{ wt %}$; the silica host is thermally stable up to temperatures above 1000 K (its weight is constant by increasing the temperature up to 1073 K). For ibuprofen in the analogue SBA-15, the loading was expressed as a filling degree of 27 wt %, as described in ref 10; to allow comparison with ibuprofen now incorporated in MCM, the filling degree was determined to be 32 wt %. This means that like for SBA-15, the pores are not completely filled. However, first, the filling degree is comparable with that of the SBA-15 materials and, second, is high enough to allow the observation of the molecules that are behaving bulk-like and molecules that are in interaction with the pore walls. This will be discussed in detail below.

Attenuated Total Reflectance Fourier Transform Infrared. Attenuated total reflectance fourier transform infrared (ATR-FTIR) spectroscopy was used to take evidence of how ibuprofen interacts with the pore walls. The spectra were recorded by a Thermo-Nicolet, Nexus 670 spectrometer at room temperature. The measurements were carried out in the wavenumber range from 400 to 4000 cm^{-1} , accumulating 128 scans having a resolution of 4 cm^{-1} .

The FTIR spectrum of MCM loaded with ibuprofen is shown in Figure 3. The spectrum of crystalline ibuprofen is included for comparison, presenting an absorption band at 1717 cm^{-1} corresponding to the carbonyl-stretching vibration in hydrogen-bonded aggregates ($1700\text{--}1725\text{ cm}^{-1}$)²⁴ that are known to be dimers in racemic crystalline ibuprofen from X-ray diffraction analysis.^{19,20} For ibuprofen confined to MCM, this band undergoes a shift toward lower wavenumbers, 1709 cm^{-1} , indicating a weakening of the C=O bond, as observed by infrared spectroscopy for ibuprofen confined in SBA¹⁰ and MCM-41⁵ and for supercooled ibuprofen as well.²¹ This indicates that ibuprofen inside of MCM pores is in the supercooled state at room temperature, which is in accordance with solid-state NMR observations that evidenced that

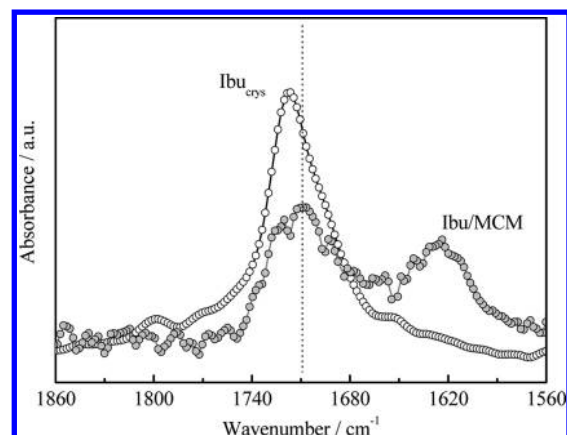


Figure 3. ATR-FTIR spectra of ibuprofen confined to MCM, Ibu/MCM, compared with bulk crystalline ibuprofen, Ibu_{crys}, at room temperature. The dotted vertical line indicates the wavenumber position of the maximum for Ibu/MCM that undergoes a shift toward lower wavenumbers relative to Ibu_{crys}. The spectrum obtained for Ibu/MCM is more or less similar to that observed for bulk amorphous ibuprofen.^{10,21}

ibuprofen molecules when confined in MCM or SBA silica matrixes are not in a solid state, either crystalline or amorphous glass, being extremely mobile, exhibiting a liquid-like behavior.^{11–14}

DRS. The complex dielectric function $\epsilon^*(f) = \epsilon'(f) - i\epsilon''(f)$, where f is the frequency of the applied oscillating electrical field and ϵ' and ϵ'' are the real part and imaginary (loss) components ($i = (-1)^{1/2}$ is the imaginary unit), was measured from 10^{-1} to 10^7 Hz using a high-resolution ALPHA analyzer supplied by Novocontrol, Hundsangen, Germany, interfaced to an active sample head. Samples were prepared in parallel plate geometry between two gold-plated electrodes with a diameter of 10 mm. The samples were previously cooled to 153 K with a rate of $10\text{ K}\cdot\text{min}^{-1}$. Dielectric spectra were collected isothermally from 153 to 373 K in increasing steps of 2 K followed by a second run of isothermal measurements upon cooling in decreasing temperature steps of 2 K in the range of 373–159 K. All isothermal measurements were carried out with an uncertainty in temperature of $\pm 0.1\text{ K}$.

Dielectric Data Analysis. To analyze the isothermal dielectric data, the model function introduced by Havriliak–Negami was fitted to both the imaginary and the real parts of the complex permittivity. Because multiple peaks are observed in the available frequency window, a sum of HN functions was employed

$$\epsilon^*(f) = \epsilon_\infty + \sum_j \frac{\Delta\epsilon_j}{[1 + (i\omega\tau_{\text{HN}j})^{\alpha_{\text{HN}j}}]^{\beta_{\text{HN}j}}} \quad (1)$$

where j is the index over which the relaxation processes are summed, $\Delta\epsilon$ is the dielectric strength, τ_{HN} is the characteristic HN relaxation time, and α_{HN} and β_{HN} are fractional parameters ($0 < \alpha_{\text{HN}} < 1$ and $0 < \alpha_{\text{HN}}\beta_{\text{HN}} < 1$) describing the symmetric and asymmetric broadening of the complex dielectric function, respectively.²⁵ From the estimated values of τ_{HN} , α_{HN} , and β_{HN} parameters, a model-independent relaxation time, $\tau = 1/(2\pi f_{\text{max}})$, was calculated according to^{25–27}

$$\tau = \tau_{\text{HN}} \times \left[\frac{\sin\left(\frac{\alpha_{\text{HN}}\beta_{\text{HN}}\pi}{2 + 2\beta_{\text{HN}}}\right)}{\sin\left(\frac{\alpha_{\text{HN}}\pi}{2 + 2\beta_{\text{HN}}}\right)} \right]^{1/\alpha_{\text{HN}}} \quad (2)$$

Close to the glass transition temperature, the temperature dependence can be described by the well-known VFTH equation,^{28–30} which reads

$$\tau(T) = \tau_{\infty} \exp\left(\frac{B}{T - T_0}\right) \quad (3)$$

where τ_{∞} and B are constants and T_0 is the so-called Vogel temperature.

Molecular Dynamic Simulations. Molecular dynamic (MD) simulations of racemic ibuprofen confined in amorphous silica have been performed using the DL POLY program.³¹ The all-atom OPLS force field³² has been employed to model the intra- and intermolecular interactions of ibuprofen molecules. The total number of molecules is $N = 104$, and it is a 50:50 mixture of each ibuprofen enantiomers R and S. The starting conformation of the R and S enantiomers was taken from the neutron diffraction determination of the crystalline racemic ibuprofen.²⁰ The length of all covalent bonds was kept fixed using the SHAKE algorithm,³³ with a relative tolerance of 10^{-8} . A 1 fs time step was used to integrate the equations of motion with the Verlet leapfrog algorithm.³⁴ A cutoff radius of 10 Å was used to account for van der Waals and electrostatic interactions. A Lennard-Jones potential was employed to represent van der Waals interactions, and Lorentz–Berthelot mixing rules were used for cross-interaction terms. Electrostatic interactions were handled by a damped shifted forces method.³⁵

The initial configuration of ibuprofen confined in an amorphous silica matrix was generated similarly as described in the MD simulations of glycerol confined to nanoporous silica channels of MCM-41 type carried out by one of us,³⁶ therefore, only the essential details are given here. The amorphous silica matrix was created from a fully relaxed atomic configuration of vitreous silica in a cubic cell of length 7.2 nm.³⁷ First, a cylindrical pore of diameter 3.6 nm along the z -axis of the silica cell was carved. Second, silicon atoms at the pore surface were removed, and oxygen dangling bonds were saturated with hydrogen atoms to form surface silanol groups. The resulting inner surface density of silanol groups was about 7.5 nm^{-2} , in fair agreement with real highly hydrated silicate surfaces.³⁸ In the present silica model, the position of silicon and oxygen atoms are fixed, while the silanol hydrogen's are allowed to rotate about the Si–O bond axis. The Si–O–H angle of the silanol groups is also constrained using a harmonic bending interaction (see data in ref 36). van der Waals interaction parameters for silica were taken from reference.³⁹ The model leads to a hydrophilic and realistic cylindrical channel of silica of mean diameter $D = 3.6 \text{ nm}$ and length $a = 7.2 \text{ nm}$, which mimics MCM-41 mesoporous materials.⁴⁰ Finally, a fully relaxed configuration of amorphous ibuprofen molecules was inserted in the generated straight cylindrical channel carved in the matrix of amorphous silica. Lorentz–Berthelot mixing rules have been used for van der Waals cross-interaction terms between ibuprofen molecules and silica.

MD simulations were performed in the NVT ensemble (constant number of particles, volume, and temperature). The density of confined ibuprofen is about 1 g cm^{-3} , in fair agreement with the results reported in the literature⁴¹ for bulk

amorphous ibuprofen. The investigated temperatures were kept constant during a given simulation using a Hoover thermostat⁴² with a relaxation time of 0.2 ps.

RESULTS AND DISCUSSION

As analyzed above, ATR-FTIR provided first evidence that ibuprofen exists inside of pores at room temperature in the supercooled state. In order to confirm this observation and to evaluate its thermal response, dielectric measurements were carried out over two runs (see the Experimental Section); the first one was to eliminate water and solvent residues. This can be seen in the isochronal plot of the real part of the complex permittivity, as illustrated in Figure 4, where ϵ' is taken at 1 kHz. A similar behavior is observed for ibuprofen encapsulated in SBA-15.¹⁰

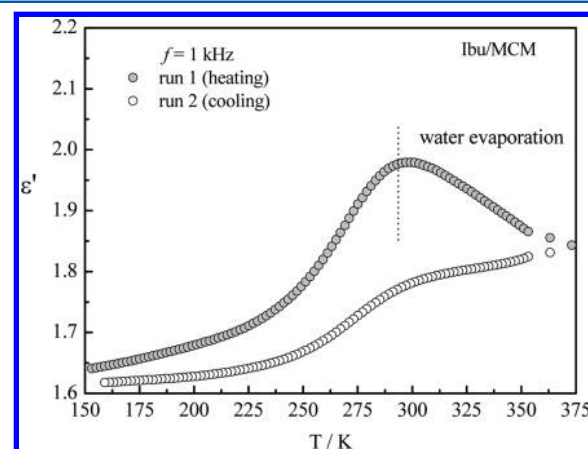


Figure 4. Temperature dependence of the real part of the complex dielectric function, ϵ' (isochronal plot at 1000 Hz for confined ibuprofen, Ibu/MCM; data obtained upon heating, run 1 (gray circles), and upon the subsequent cooling, run 2 (open circles). Data were taken from isothermal measurements carried out between 153 and 373 K. The vertical dashed line indicates the temperature above which water evaporation occurs in the as-prepared Ibu/MCM sample.

Water evaporation gives the origin to the broad peak in the $\epsilon'(T)$ trace centered at around 300 K, at this particular frequency. In the second run, a step-like behavior is observed, as usually found when a relaxational process occurs and as already found for Ibu/SBA-15.¹⁰ No signs of crystallization or melting were detected over all of the temperature range studied ($\Delta T \approx 200 \text{ K}$). This is in agreement with NMR studies³ in which it was concluded that nucleation of crystallites inside of a 3.5 nm pore diameter (MCM-41) is not possible; also, in a silica matrix (SBA-15) with a pore diameter of 8.6 nm, no crystallization was observed.¹⁰ This confirms that ibuprofen is amorphous inside of pores and does not undergo those phase transitions under the thermal treatment to which it is submitted. Furthermore, the absence of bulk-like melting indicates that no residual crystallized bulk amorphous ibuprofen exists outside of the pores; this means that efficient removal during the washing step was carried out. Measurements taken 2 years later confirm that ibuprofen still exists as an amorphous material inside of MCM.

Data collected in the second run is taken for further analysis and discussion. It must be noted that the dielectric loss of the dried MCM matrix is negligible compared to that observed for the filled matrix; therefore, the detected dielectric response for

the Ibu/MCM composite is dominated by the response of ibuprofen molecules.

Figure 5 presents the loss peaks for confined ibuprofen at three representative temperatures where multiple relaxation

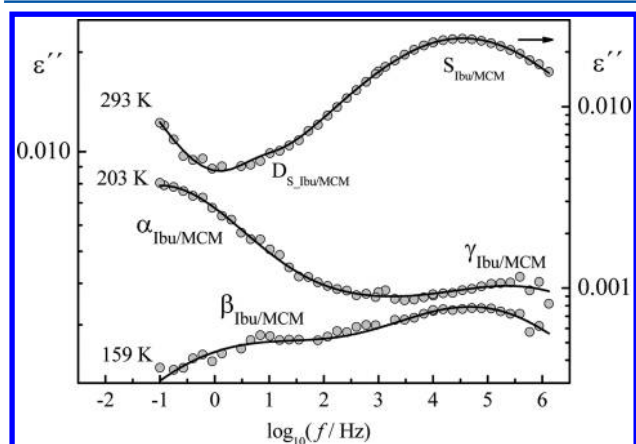


Figure 5. Dielectric loss versus frequency at the indicated temperatures for ibuprofen confined to MCM (pore diameter of 3.6 nm, Ibu/MCM). The solid lines are the overall HN fit to data using eq 1.

processes can be observed, as already discussed for bulk amorphous ibuprofen²¹ and when confined to SBA.¹⁰ At the lowest temperature (159 K), two secondary processes with a weak intensity are observed, which have similar features to the γ and β processes observed for the bulk amorphous ibuprofen. Therefore, a similar labeling is applied for Ibu/MCM, $\gamma_{\text{Ibu/MCM}}$ and $\beta_{\text{Ibu/MCM}}$. With increasing temperature (203 K), these processes due to localized fluctuations are followed by a more intense process attributed to the dynamic glass transition process of the confined guest, the $\alpha_{\text{Ibu/MCM}}$ process. At even higher temperatures (293 K), a further relaxation process is observed, becoming the dominating mode in the dielectric spectra but carrying at its low-frequency tail a weak process. These two processes are detected at lower frequencies (higher temperatures) relative to the $\alpha_{\text{Ibu/MCM}}$ process (dynamic glass transition). A similar behavior was observed for ibuprofen confined to a comparable mesoporous matrix (SBA), in which two additional processes are also observed compared to the bulk amorphous material.¹⁰ These modes were designated as the surface process ($S_{\text{Ibu/MCM}}$) assigned to guest molecules interacting with the pore surface of the host^{43–45} and the Debye process ($D_{\text{Ibu/MCM}}$) associated with the dynamical behavior of the molecules that relax according to the surface process.¹⁰

The comparison with bulk amorphous ibuprofen by an isochronal plot (Figure 6) confirms the assignment of the different relaxation processes and the existence of the two additional S and D relaxations.

For sake of clearness, in a first paragraph, the bulk-like relaxations will be considered followed by an analysis of those processes that are not characteristic of the bulk, $S_{\text{Ibu/MCM}}$ and $D_{\text{Ibu/MCM}}$ processes.

Bulk-Like Processes in Ibu/MCM. Figure 6 shows the shift in location of the $\beta_{\text{Ibu/MCM}}$ and $\alpha_{\text{Ibu/MCM}}$ processes to lower temperatures compared to bulk amorphous ibuprofen. This is confirmed by the analysis of the isotherms, as detailed in Figure 7a and b, where also the $\gamma_{\text{Ibu/MCM}}$ process is seen. The temperature at which the dielectric loss is plotted in Figure 7a, $T = 203$ K, corresponds to the subglass region in bulk

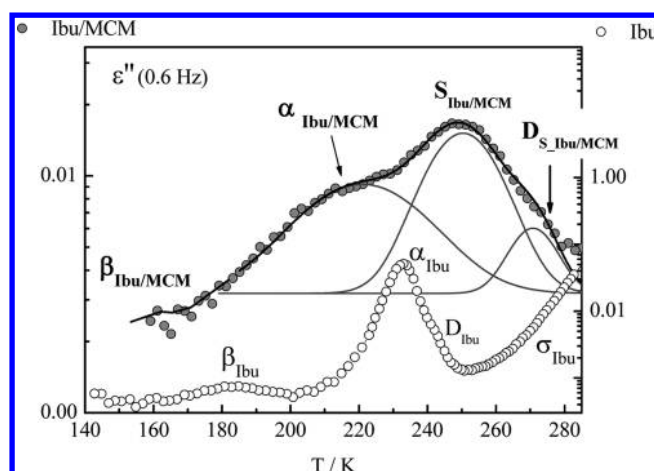


Figure 6. Dielectric loss of ibuprofen versus temperature at a frequency of 0.6 Hz confined to the MCM mesopores (solid circles) taken from isothermal data in comparison to the bulk amorphous (open circles).²¹ The solid lines are the three Gaussians summed to simulate the isochronal plot of Ibu/MCM above 170 K.

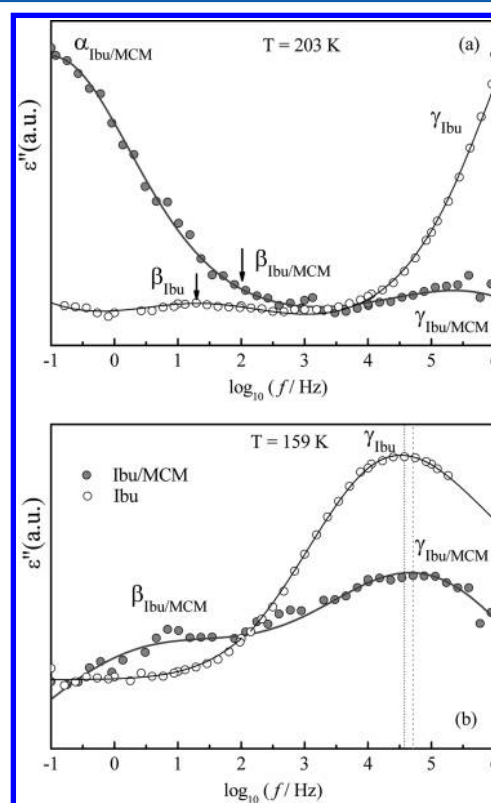


Figure 7. Dielectric loss versus frequency for ibuprofen confined to MCM in comparison with bulk amorphous ibuprofen at the indicated temperatures: (a) close to the glass transition of Ibu/MCM and (b) in the subglass region, showing in more detail the influence of confinement on the bulk-like relaxations. In both figures, the solid lines are the overall HN fits to the corresponding loss data where a sum of HN functions was assumed.

amorphous ibuprofen for which the α process is not detected. However, in contrast, the α process for Ibu/MCM, $\alpha_{\text{Ibu/MCM}}$ is coming into the frequency window at this temperature, indicating a decrease in the dynamic glass transition temperature for confined ibuprofen, evidencing a higher mobility of ibuprofen molecules inside of the MCM pores. This is also the

case for the secondary $\beta_{\text{Ibu/MCM}}$ process (the relative position to the bulk indicated by the arrows).

Therefore, the comparison with bulk amorphous ibuprofen clearly reveals the influence of incorporation in MCM as a true confinement effect.

Furthermore, the secondary $\gamma_{\text{Ibu/MCM}}$ process seems to be slightly slower at 203 K relative to the respective process in bulk amorphous ibuprofen, undergoing some influence of the $\beta_{\text{Ibu/MCM}}$ relaxation. The detection of the β process for confined Ibu at 159 K, deeper in the subglass region (Figure 7b), against its absence at this temperature in bulk amorphous Ibu, confirms the higher mobility of ibuprofen molecules when incorporated in MCM. At this temperature, the $\gamma_{\text{Ibu/MCM}}$ is slightly more mobile relative to the bulk (the relative positions are indicated by the dashed lines); this points out a different activation energy for this secondary relaxation under confinement compared with that of the bulk; these features will be commented on further. In both figures, the solid lines are the overall HN fits to the loss data, where a sum of individual HN functions (eq 1) was assumed. The respective fitting parameters are presented in Table 1.

Table 1. Shape Parameters, α_{HN} and β_{HN} , for the Fit Obtained by a Sum of Havriliak–Negami Functions (Equation 1) for the Individual Bulk-Like Processes Detected in Ibu/MCM

process	α_{HN}	β_{HN}
$\gamma_{\text{Ibu/MCM}}$	0.3	0.9
$\beta_{\text{Ibu/MCM}}$	0.25	1
$\alpha_{\text{Ibu/MCM}}$	0.50 ± 0.08	1

Figure 7 shows the secondary relaxations that are not commonly observed in low-molecular-weight glass formers under confinement.^{8,46} This becomes also evident in the relaxation map presented in Figure 8; the relaxation times τ_{HN} were extracted from the HN fit (eq 1) and converted to the model-independent relaxation time, τ , according to eq 2.

In the subglass region, as expected for localized fluctuations, the temperature dependence of relaxation times of the secondary processes follows an Arrhenius law, $\tau(T) = \tau_{\infty} \exp(E_a/RT)$, where τ_{∞} is the pre-exponential factor, E_a is the activation energy, R is the ideal gas constant, and T is the temperature. The respective τ_{∞} and E_a parameters are presented in Table 2.

Interestingly, the extrapolation of the $\gamma_{\text{Ibu/MCM}}$ trace goes toward the one of the high temperature branch of the bulk α process, which gives origin to the a process close to the melting temperature, T_m ($T_{m,\text{Ibu-bulk}} = 347 \text{ K}$; $1/T = 0.002882 \text{ K}^{-1}$).²¹ This is confirmed by the coincidence of the two prefactors, the one obtained from the temperature dependence of $\tau_{\alpha,\text{Ibu}}$ at the highest temperatures following a VFTH law (VFTH₂ in ref 21) and the one determined from the Arrhenius equation of the $\tau_{\gamma,\text{Ibu/MCM}}$ respectively $(1.7 \pm 0.1) \times 10^{-12}$ and $(2 \pm 1) \times 10^{-12} \text{ s}$. This can be taken as an indication that the equilibrium liquid state of the confined ibuprofen is thermodynamically equivalent to that of the bulk liquid.

Moreover, the $\tau_{\gamma,\text{Ibu}}$ of bulk amorphous ibuprofen bends off toward the $\tau_{\alpha,\text{Ibu}}$ above T_g ,²¹ with the respective relaxation times being longer than the ones obtained by extrapolating the glassy state Arrhenius dependence. A rationalization of this behavior is given in ref 46 as being a hybridization of the γ with the β relaxation, which reflects a transference of the β process

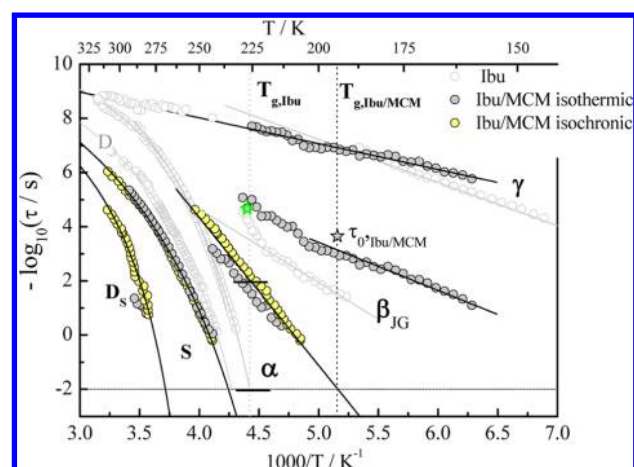


Figure 8. Relaxation time, τ , versus $1000/T$ for the processes detected in Ibu/MCM (filled circles) in comparison with bulk Ibu (open circles): gray symbols, relaxation times obtained from isothermal loss data collected during cooling for the confined sample; yellow symbols, τ obtained from the isochronal plots ($\epsilon''(T; f = \text{const})$); $\tau = 1/(2\pi f)$; $1/T_{\text{max}}$. Lines are fits of the Arrhenius and VFTH equation to the corresponding temperature dependence. Vertical dotted lines indicate the dielectric glass transition temperatures for bulk and confined ibuprofen T_g^{diel} ($\tau_{\alpha} = 100 \text{ s}$). The light gray star indicates the primitive relaxation time, τ_0 , estimated from the Coupling Model (CM) (eq 4) for confined ibuprofen at $T_{g,\text{Ibu/MCM}} = 194 \text{ K}$, and the green star is τ_0 estimated for bulk amorphous ibuprofen at $T_{g,\text{Ibu,bulk}} = 226 \text{ K}$; the short horizontal bars along $T_{g,\text{bulk}}$ indicate the $\log(\tau)$ distance at bulk T_g to the τ_0 value at this same temperature.

properties to the γ process. It was demonstrated that the bulk β relaxation is the so-called JG process,^{47,48} β_{JG} , or the primitive relaxation process, a precursor of the α relaxation, as postulated in the framework of the CM.⁴⁹

The apparent change of the $\beta_{\text{Ibu/MCM}}$ trace to a higher slope at the highest temperatures upon approaching the $\alpha_{\text{Ibu/MCM}}$ trace seems to support the attribution to a JG process, as found for the bulk.

In the framework of the CM by Ngai, a relationship of the (primitive) relaxation time of the JG process and the relaxation time of the α process is predicted. If this relationship is valid, a change in the relaxation time of the JG process will be also related to a change in the relaxation time of the α mode. Because of the fact that the confinement changes both the α and the β relaxation, the validity of the CM can be checked. The relaxation time of the JG process, $\tau_{\beta,\text{JG}}$, and that of the α process are interrelated in the framework of the CM through the equation⁴⁹

$$\tau_{\text{JG}}(T) \approx \tau_0(T) = t_c^n [\tau_{\alpha}(T)]^{1-n} \quad (4)$$

where τ_0 is the primitive relaxation time of the CM, n is the coupling parameter, t_c is a time characterizing the crossover from independent to cooperative fluctuations found to be close to $2 \times 10^{-12} \text{ s}$ for molecular glass formers,⁵⁰ $\tau_{\alpha} = \tau_{\text{KWW}}$ is the relaxation time of the Kohlrausch–Williams–Watts (KWW) function,^{51–53} $\phi(t) = \exp[-(t/\tau_{\text{KWW}})^{\beta_{\text{KWW}}}]$ that describes the relaxation spectra in the time domain; $0 < \beta_{\text{KWW}} < 1$; $\beta_{\text{KWW}} = 1$ for a Debye response. The coupling parameter is defined by $1 - \beta_{\text{KWW}}$, where β_{KWW} is estimated by the HN shape parameters of the $\alpha_{\text{Ibu/MCM}}$ process (Table 1) using the empirical correlation ($\beta_{\text{KWW}} = (\alpha_{\text{HN}} \cdot \beta_{\text{HN}})^{1/1.23}$) proposed by Alegria et al.^{54,55} From this expression, a value of $\beta_{\text{KWW}} = 0.57$ is obtained, from which eq 4 gives a value of $\tau_{\text{JG}} \approx \tau_0$ at $T_{g,\text{diel}}$ of 1.25×10^{-4}

Table 2. Pre-exponential Factor and Activation Energy from the Arrhenius Equation for the Bulk-Like Processes Detected in Ibuprofen Confined to MCM and SBA^a

system	γ process		β process		α process	
	τ_{∞}/s	$E_a/kJ\ mol^{-1}$	τ_{∞}/s	$E_a/kJ\ mol^{-1}$	τ_{∞}/s	$E_a/kJ\ mol^{-1}$
Ibu/MCM	$(2 \pm 1) \times 10^{-12}$	18.2 ± 0.6	$(5 \pm 3) \times 10^{-13}$	34 ± 1	$(7 \pm 6) \times 10^{-27}$	104 ± 4
Ibu/SBA	$(8 \pm 5) \times 10^{-13}$	20.0 ± 0.6	$(9 \pm 4) \times 10^{-13}$	34 ± 1	$(5 \pm 4) \times 10^{-30}$	122 ± 10
Ibu _{bulk} ²¹	$(6 \pm 4) \times 10^{-16}$	30.5 ± 0.7	$(3 \pm 4) \times 10^{-16}$	52 ± 2	$E_{a,app}(T_g) = 400 \pm 20^b$	

^aFor the α process, the parameters were taken from the linear regression of both isothermal and isochronal sets of data. Data for bulk amorphous ibuprofen were included for comparison. ^bApparent activation energy calculated using the parameters of the VFTH₁ equation fitted to the α relaxation of bulk amorphous ibuprofen (see ref 21 for details).

s for the confined system. This is in good agreement with the experimental τ_{β} value at 194 K; see the green star in Figure 8. Therefore, also for the confined system, the β secondary process is identified as being the JG relaxation. The attribution to a JG relaxation can be also confirmed by testing the ratio $E_{a,\beta}/RT_g$, where $E_{a,\beta}$ is the activation energy of the JG β relaxation in the glassy state, T_g is the dielectric glass transition temperature estimated at $\tau_{\alpha} = 100$ s, and R is the gas constant, which gives 21 for Ibu/MCM, close to $E_a/RT_g = 24$ as proposed by Kudlik et al.⁵⁶ and found for several glass formers.⁵⁷

Of interest is the finding that both $\gamma_{Ibu/MCM}$ and $\beta_{Ibu/MCM}$ relaxations undergo less accentuated changes with increasing temperature upon crossing T_g , relative to the bulk. For ibuprofen confined to 8.6 nm pores (SBA matrix), an intermediate behavior is found upon passing T_g , namely, the bending of the β trace upon approaching the α trace, exhibiting a similar behavior to Ibu/MCM in the glassy state (see Figure 9). At temperatures above $T_{g,bulk}$, the relaxation times of all of

that presents a pronounced VFTH law dependence.²¹ The linearity in this temperature range is confirmed by the analysis of the isochronal ϵ'' plots that were carried out due to an ill definition of the isothermal loss curves. A superposition of k Gaussians⁵⁸ was fitted to the isochronal representation for each measured frequency (see Figure 6) to obtain the maximum temperature of peaks, $T_{max,k}$; this gives a linear dependence for $\alpha_{Ibu/MCM}$ (yellow circles in Figure 8). The respective parameters of the Arrhenius equation given in Table 2 correspond to the linear regression of the two sets of data (isothermal and isochronal). The same analysis gave the temperature dependence of relaxation times for the $S_{Ibu/MCM}$ and $D_{Ibu/MCM}$ processes, which will be discussed in the next section; however, it is worthwhile to note for the latter processes how data obtained from the isochronal deconvolution superimpose/get real close with/to the values extracted from isothermal fit of dielectric loss, validating this analysis.

The Arrhenius dependence of the relaxation times for $\alpha_{Ibu/MCM}$ close to its glass transition and the respective shift toward lower temperatures/higher frequencies means that (i) it exhibits a much faster dynamics than that in the bulk, as previously mentioned upon analyzing the isothermal raw data, and (ii) the pore diameter, 3.6 nm, is a dimension that already interferes with the length scale inherent to the cooperative motion underlying the bulk process. However, the prefactor, τ_{∞} , of the Arrhenius law for the confined system is unphysically low ($\sim 10^{-26}$ s) compared with the typical values of 10^{-12} – 10^{-14} s for local orientational fluctuations, which is rationalized as an indication that some degree of cooperativity still affects the glass transition dynamics also supported by a relatively high value of activation energy ($104\ kJ\ mol^{-1}$). For ibuprofen confined to a larger pore size (8.6 nm, SBA-15 matrix), both the prefactor ($\sim 10^{-30}$ s) and activation energy ($122\ kJ\ mol^{-1}$) indicate an increased degree of cooperativity. For bulk amorphous ibuprofen, the curvature of the temperature dependence of the relaxation times shows the underlying cooperative nature of the α process. The apparent activation energy at $T_{g,bulk}$ (226 K) is even higher ($400\ kJ\ mol^{-1}$). These observations are in line with the results reported in ref 59 for poly(methyl phenyl siloxane) (PMPS) confined to nanoporous glasses for pore sizes of 5 and 2.5 nm, indicating also for Ibu/MCM the manifestation of finite size effects. Nevertheless, while for 2.5 nm a single low activation energy process ($38\ kJ\ mol^{-1}$) is observed for PMPS,⁵⁹ for Ibu confined in MCM and SBA, both the α process and its precursor, the β_{JG} process, are still detected. According to the theoretical CM approach, when n decreases, the same happens with the separation between the α relaxation and the β_{JG} process and, in the limit of extreme confinement when the size becomes smaller than the length scale of the α process, that is, when $n \rightarrow 0$, $\tau_{\alpha} \rightarrow \tau_0 \approx \tau_{JG}$ and the α relaxation is transformed into the JG relaxation.^{46,60} For

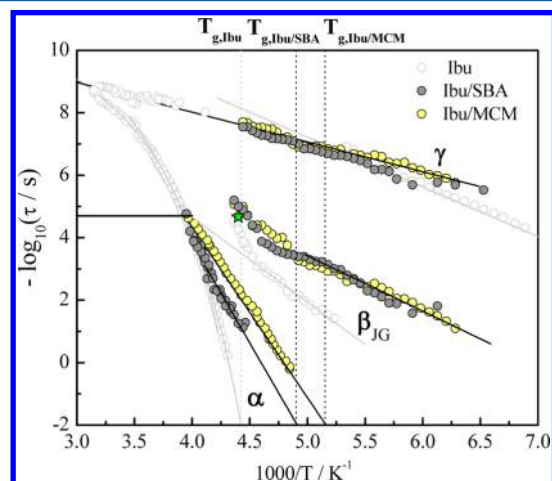


Figure 9. Comparison of the temperature dependence relaxation times of the α , β , and γ processes for both 3.6 (MCM) and 8.6 (SBA) nm pores with that of the bulk: open circles, bulk; gray filled circles, Ibu/SBA-15; yellow filled circles, Ibu/MCM-41. Lines are fits of the Arrhenius and VFTH formulas to the corresponding data.

the β_{JG} processes, bulk or confined to 8.6 and 3.6 nm pores, merge together at the primitive relaxation time of the CM, τ_0 , estimated for bulk amorphous ibuprofen (star in Figure 9).

At higher temperatures, the relaxation map presents the temperature dependence of the relaxation times extracted from the fit of loss data collected isothermally for the α process of Ibu/MCM. Interestingly, $\tau_{\alpha,Ibu/MCM}(1/T)$ at the lowest temperatures at which it is detected follows an Arrhenius-like behavior, contrary to what was observed for bulk amorphous ibuprofen

ibuprofen confined in MCM, $n = 0.43$, which is smaller than $n = 0.48$ as found for bulk ($\beta_{\text{KWW}} = 0.52$),²¹ and the respective separation of the α and β traces in the relaxation map is smaller relative to bulk at the respective T_g 's. This can be seen also by comparing the relaxation times of the α process at the bulk glass transition (226 K). In fact, $\tau_{\alpha,\text{Ibu/MCM}}$ is reduced relative to $\tau_{\alpha,\text{Ibu-bulk}}$ at $T_{g,\text{bulk}}$ by about 4 decades, approaching the value of bulk τ_0 ($\tau_{0,\text{Ibu-bulk}}$) indicated by the green star in Figure 8; the short horizontal bars along $T_{g,\text{bulk}}$ in Figure 8 indicate the distance in $\log(\tau)$ between the relaxation time of the α process and $\tau_{0,\text{Ibu-bulk}}$, being much shorter for $\alpha_{\text{Ibu/MCM}}$. This points to confined ibuprofen as a suitable system to observe the predicted limit when $n \rightarrow 0$, which should be reached upon further decrease of the pore size.

The manifestation of size effects can also be discussed by considering the pore diameter dependence of the glass transition temperature. Taking the temperature where the relaxation time is $\tau = 100$ s,^{61,62} the extrapolation of the linear temperature dependence of $\tau_{\text{Ibu/MCM}}$ gives a value of $T_{g,\text{Ibu/MCM}} = 194$ K. Compared with bulk amorphous ibuprofen ($T_g = 226$ K),²¹ a T_g depression of 32 K is observed for ibuprofen confined to MCM (3.6 nm), greater than the 22 K decrease found for ibuprofen confined to SBA-15 ($T_g = 204$ K) with a higher pore size (8.6 nm).¹⁰ The decrease in the glass transition temperature and the mobility enhancement with the pore size decrease is illustrated in Figure 9 through a scale up of the activation plot close to the glass transition regions in which the temperature dependence for ibuprofen confined in SBA is included. Figure 10 illustrates the same effect for the glass transition temperature determined from the DRS results against the inverse of the pore size, $1/d$; for bulk amorphous ibuprofen, $1/d = 0$.

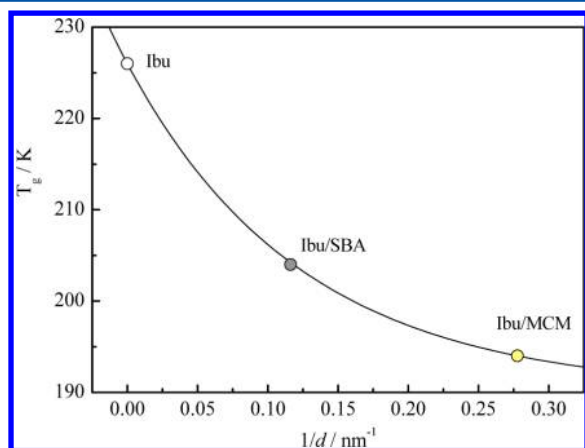


Figure 10. Glass transition temperature determined from dielectric data versus the inverse of the pore diameter for ibuprofen in 3.6 (MCM) and 8.6 (SBA) nm pores; the T_g value for bulk liquid ibuprofen is also included ($1/d = 0$).

Due to the incoming of the surface process that will be analyzed in the next section, it was not possible to distinguish the $\alpha_{\text{Ibu/MCM}}$ process and extract the respective relaxation times at higher temperatures, but probably, it will collapse into the $\alpha_{\text{Ibu,bulk}}$ trace, as observed for Ibu/SBA¹⁰ and found for the secondary relaxations as well.

It is interesting to note the change from a VFTH to an Arrhenius-like temperature dependence in the confined systems relative to bulk amorphous ibuprofen at the lowest temper-

atures. This occurs at $\sim 2 \times 10^{-5}$ s, which is the relaxation time at which the extrapolation of the glassy state Arrhenius temperature dependence of the $\beta_{\text{Ibu,bulk}}$ relaxation intercepts the $\alpha_{\text{Ibu-bulk}}$ trace (see Figure 9), taken as the onset of significant increase of intermolecular cooperativity in the framework of the CM^{46,63,64} and previously discussed for bulk amorphous ibuprofen.²¹

$S_{\text{Ibu/MCM}}$ and $D_{S,\text{Ibu/MCM}}$ Processes. For the confined system, the S process is observed at lower relaxation times/higher temperatures than the $\alpha_{\text{Ibu/MCM}}$ process, as found for Ibu/SBA.¹⁰ Similar processes have been found for confined guests interacting with the pore surface of the host.^{10,23,43–45,65} Therefore, its molecular origin in Ibu/MCM is also assigned with molecular fluctuations of the ibuprofen molecules adsorbed at the pore walls. To confirm this attribution, the temperature dependence of the dielectric strength for the S process is plotted in Figure 11 together with the variation for

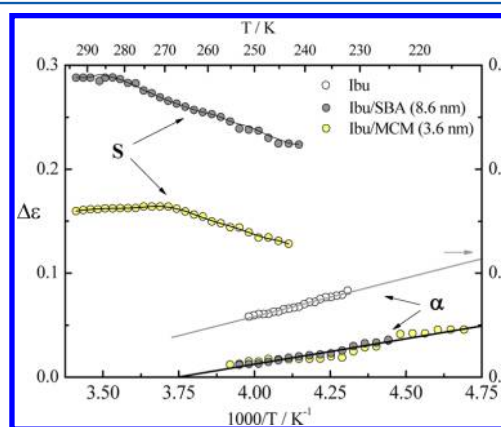


Figure 11. Temperature dependence of the dielectric strength, $\Delta\epsilon$, for the α and S process for ibuprofen confined in MCM and SBA mesoporous silica matrices (left-hand axis). $\Delta\epsilon$ for the α relaxation of bulk amorphous ibuprofen is shown for comparison (right-hand axis).

the α process for confined ibuprofen in both MCM and SBA matrixes. Indeed, $\Delta\epsilon_{S,\text{Ibu/MCM}}$ shows, in general, an identical temperature dependency as the one obeyed by the analogous S process found in Ibu/SBA. The nonmonotonous variation was explained as a counterbalance of two effects; at the lowest temperatures, the increase of $\Delta\epsilon(T)$ is caused by a weakening with the temperature increase of the interaction of ibuprofen molecules with the pore wall, which leads to the reorientation of greater parts of the molecular dipole vector (increased fluctuation angle) and/or an increased number of fluctuating dipoles as observed for the S process detected in E7 confined in the same kind of hosts;²³ at the highest temperatures, $\Delta\epsilon$ follows the predicted decrease with the temperature increase due to thermal energy (Onsager–Kirkwood–Fröhlich equation).^{66–68}

The $\Delta\epsilon$ temperature dependence in Figure 11 also acts as a confirmation of the assignment of the bulk-like α process for confined ibuprofen because its dielectric strength decreases with the temperature increase, recognized as a characteristic sign of the α relaxation detected in conventional glass formers and polymers.⁶⁹ Is interesting to note that the magnitude of the dielectric strength of the bulk-like α process is identical for ibuprofen confined in MCM and SBA mesopores. Because the dielectric strength is proportional to the volume density of dipoles,^{66,67} this pulls apart the hypothesis of a less dense

packing of ibuprofen molecules in the middle of the MCM pores as the origin of the mobility enhancement of Ibu/MCM relative to Ibu/SBA. This strengthens the conclusion that the reduction on the glass transition temperature is a real consequence of finite size effects upon decreasing the pore size.

The simultaneous observation of a α relaxation and an S process allows classification of the dynamics of confined ibuprofen molecules into two fractions, one liquid-like due to molecules close to the pore center with relaxation rates faster than the bulk guest and another due to molecules interacting with the pores with significantly hindered mobility.

The respective activation plot (see Figure 8) presents the curvature characteristic of cooperative processes; therefore, the S process is assigned to the dynamic glass transition of the ibuprofen molecules (e.g., monomers, linear dimers) weakly adsorbed in the pore walls. The incorporation of ibuprofen molecules in MCM-41 3.6 nm pores was simulated by MD (see the details in the Experimental Section) from which a top view of a simulation cell is shown in the top part of Figure 12. The

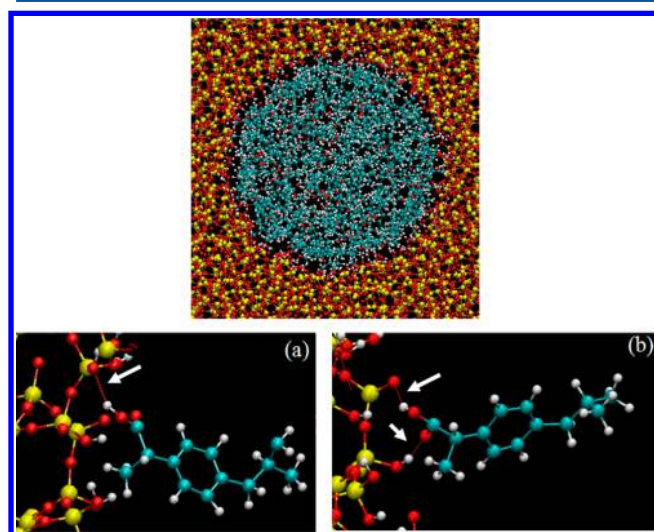


Figure 12. The upper part shows the top view of a simulation cell obtained by MD simulations of ibuprofen confined in a completely filled cylindrical pore of 3.6 nm diameter that mimics MCM-41 mesoporous materials; the lower part represents a zoom of the simulation cell illustrating the interaction of the carboxylic group of ibuprofen with the silanol groups through (a) one hydrogen bond and (b) two hydrogen bonds identified by the white arrows.

figure also illustrates the interaction between the ibuprofen COOH moiety and the surface silanol groups via one (Figure 12a) or two (Figure 12b) hydrogen bonds. The mobility of ibuprofen molecules in the inner surface layer adjacent to the cylindrical channel of silica gives rise to the S process, while the reorientational motions of molecules in the core of the pore cavity are responsible by the $\alpha_{\text{Ibu/MCM}}$ process.

A VFTH equation was fitted to the temperature dependence of the relaxation times of this S process (solid line in Figure 8) with the following parameters $\tau_{\infty} = 3.1 \times 10^{-13}$ s, $B = 1932$ K, and $T_0 = 178$ K, allowing one to estimate a glass transition temperature ($\tau = 100$ s) of 236 K, lying ~ 42 K above the glass transition estimated from dielectric data of the $\alpha_{\text{Ibu/MCM}}$ process. For Ibu/SBA $T_{\text{g,S}} = 231$ K lying 27 K above $T_{\text{g},\alpha_{\text{Ibu/SBA}}}$, the increase in $\Delta T_{\text{g}} (=T_{\text{g,S}} - T_{\text{g},\alpha})$ is higher for the lower pore size due to a greater effect upon lowering T_{g} .

Finally, at the high-temperature flank of the S process as seen in the isochronal representation (Figure 6), a further relaxation process with a weak intensity is observed, designated as the $D_{\text{S,Ibu/MCM}}$ process, also detected for Ibu/SBA¹⁰ and discussed for bulk amorphous ibuprofen.²¹

For bulk amorphous ibuprofen, it was proposed that the dynamics of both the Debye and α process are correlated with the respective temperature dependence of relaxation times running in parallel.²¹ For the bulk-like $\alpha_{\text{Ibu/MCM}}$ relaxation, the Debye process was not detected due to the overlapping with the strong S process; the same was true for ibuprofen confined to SBA.¹⁰ Nevertheless, a Debye-shaped relaxation was detected, whose temperature dependence of the relaxation times followed the one of the $S_{\text{Ibu/MCM}}$ process (see Figure 8), being designated as the $D_{\text{S,Ibu/MCM}}$ process; the analogue process was also detected for Ibu/SBA.¹⁰ This process seems to have originated from the cis–trans conversion of the O=C–O–H group that is coupled to the interfacial hydrogen-bonded structures formed between the silanol groups and ibuprofen molecules lying in the inner surface layer. In fact, MD simulations demonstrated the coupling between the internal cis–trans conversion of the O=C–O–H group and the change of the intermolecular linear/cyclic hydrogen-bonded structures.⁷⁰ Moreover, it was demonstrated for bulk amorphous ibuprofen that the effective rotational potential energy barriers of the O=C–O–H groups due to the surroundings are averaged, and the dipolar relaxation follows a simple exponential decay responsible for the Debye-like nature of the observed relaxation peak in DRS for bulk amorphous ibuprofen²¹ and now for the confined drug.

CONCLUSIONS

The detailed dielectric characterization of the molecular mobility of ibuprofen confined to a MCM-41 silica matrix with a pore diameter of 3.6 nm is provided confirming that ibuprofen exists in the glass or supercooled state inside of pores, depending on the temperature. Multiple relaxation processes were identified, three bulk-like and two processes that were not found for bulk amorphous ibuprofen. Concerning bulk-like processes, it was possible to characterize two secondary relaxations, designated γ and β in decreasing order of frequency, whose temperature dependence follows an Arrhenius behavior as found for the respective processes in bulk amorphous ibuprofen, however with some discrepancies. The $\gamma_{\text{Ibu/MCM}}$ trace evolves with the temperature increasing with a relatively lower slope compared to the $\gamma_{\text{Ibu,bulk}}$ going toward the high-temperature $\alpha_{\text{Ibu,bulk}}$ -trace of bulk amorphous ibuprofen upon approaching T_{m} . The $\beta_{\text{Ibu/MCM}}$ process was assigned as a JG process taken as the precursor of the relaxation process responsible for the dynamical glass transition in the framework of the CM, being shifted to lower temperatures relative to the homologous process in bulk amorphous ibuprofen, giving a first indication of the lowering of the glass transition temperature. This was confirmed by the analysis of the $\alpha_{\text{Ibu/MCM}}$ process, which, in the T region at which it was detected, obeys an Arrhenius law whose extrapolation to $\tau = 100$ s gives a glass transition temperature of 194 K, representing a lowering of 32 K relative to the bulk guest. This was rationalized as 3.6 nm being a dimension that already interferes with the length scale inherent to the cooperative motion of the underlying bulk process, however with some cooperativity persisting as inferred by the low value of the exponential prefactor. The separation between the α and β traces in the

relaxation map is much smaller for the confined system (4 decades in $\log(\tau)$ at $T_{g, \text{ibu-bulk}}$) compared to that for the bulk, as expected according to the CM; however, the limit situation for which the α process is transformed into the β_{G} was not reached yet; nevertheless, confined ibuprofen exhibits finite size effects due to confinement into nanopores, being a suitable system to test this prediction. While the $T_{g, \text{ibu/MCM}}$ and $\tau_{\alpha, \text{ibu/MCM}}$ decrease indicates a higher mobility of the ibuprofen guest molecules inside of pores, the dynamics of molecules adsorbed at the pore walls that are in the origin of the so-called S process, not found in bulk amorphous ibuprofen, is highly slowed down. The coexistence of two families of molecules with different mobilities was also found for ibuprofen confined in SBA-15 with 8.6 nm of pore size, whose dynamical behavior is intermediate between the bulk and that now characterized for the 3.6 nm pore size. Additionally, at the low-frequency flank of the dominant S process, a Debye-like relaxation is found, as observed also for ibuprofen confined into SBA. This relaxation mode has been attributed to the cis–trans conversion of the O=C–O–H group that is coupled to the fluctuations of the interfacial hydrogen-bonded structures that are in the origin of the S process.

AUTHOR INFORMATION

Corresponding Author

*E-mail: natalia.correia@univ-lille1.fr.

Present Address

#A.R.B.: Jülich Centre for Neutron Science & Institute for Complex Systems, Forschungszentrum Jülich, 52425 Jülich, Germany.

Notes

The authors declare no competing financial interest.

ACKNOWLEDGMENTS

N.T.C. and A.R.B. thank the BAM Federal Institute for Materials Research and Testing for the use of its research facilities. Financial support for this work was provided through Contract PEst-C/EQB/LA0006/2011 and the Project PTDC/CTM/098979/2008 implemented within the framework of the Programme “Promover a Produção Científica, o Desenvolvimento Tecnológico e a Inovação 002: Investigação Científica e Tecnológica (3599-PPCDTI)”, financed by Fundação para a Ciência e Tecnologia (FCT), IP.

REFERENCES

- (1) Beiner, M.; Rengarajan, G. T.; Pankaj, S.; Enke, D.; Steinhart, M. Manipulating the Crystalline State of Pharmaceuticals by Nanoconfinement. *Nano Lett.* **2007**, *7*, 1381–1385.
- (2) Rengarajan, G. T.; Enke, D.; Beiner, M. Crystallization Behavior of Acetaminophen in Nanopores. *Open Phys. Chem. J.* **2007**, *1*, 18–24.
- (3) Azais, T.; Tourné-Péteilh, C.; Aussenac, F.; Baccile, N.; Coelho, C.; Devoisselle, J. M.; Babonneau, F. Solid-State NMR Study of Ibuprofen Confined in MCM-41 Material. *Chem. Mater.* **2006**, *18*, 6382–6390.
- (4) Hancock, B. C.; Shamblin, S. L.; Zografi, G. Molecular Mobility of Amorphous Pharmaceutical Solids below Their Glass Transition Temperatures. *Pharm. Res.* **1995**, *12*, 799–806.
- (5) Yoshioka, M.; Hancock, B. C.; Zografi, G. J. Inhibition of Indomethacin Crystallization in Poly(vinylpyrrolidone) Coprecipitates. *J. Pharm. Sci.* **1995**, *84*, 983–986.
- (6) Kranbuehl, D.; Knowles, R.; Hossain, A.; Hurt, M. Modelling the Effects of Confinement on the Glass Transition Temperature and Segmental Mobility. *J. Phys.: Condens. Matter* **2003**, *15*, S1019–S1029.
- (7) Leys, J.; Sinha, G.; Glorieux, C.; Thoen, J. Influence of Nanosized Confinements on 4-n-Decyl-4'-cyanobiphenyl (10CB): A Broadband Dielectric Study. *Phys. Rev. E* **2005**, *71*, 051709.
- (8) Kremer, F.; Huwe, A.; Schönhals, A.; Róžański, S. A. Molecular Dynamics in Confining Space. In *Broadband Dielectric Spectroscopy*; Schönhals, A., Kremer, F., Eds.; Springer-Verlag: Berlin, Heidelberg, Germany, 2003; Chapter 6.
- (9) Schönhals, A.; Goering, H.; Schick, Ch. Segmental and Chain Dynamics of Polymers: From the Bulk to the Confined State. *J. Non-Cryst. Solids* **2002**, *305*, 140–149.
- (10) Brás, A. R.; Merino, E. G.; Neves, P. D.; Fonseca, I. M.; Dionísio, M.; Schönhals, A.; Correia, N. T. Amorphous Ibuprofen Confined in Nanostructured Silica Materials: A Dynamical Approach. *J. Phys. Chem. C* **2011**, *115*, 4616–4623.
- (11) Izquierdo-Barba, I.; Sousa, E.; Doadrio, J. C.; Doadrio, A. L.; Pariente, J. P.; Martínez, A.; Babonneau, F.; Vallet-Regí, M. Influence of Mesoporous Structure Type on the Controlled Delivery of Drugs: Release of Ibuprofen from MCM-48, SBA-15 and Functionalized SBA-15. *J. Sol–Gel Sci. Technol.* **2009**, *50*, 421–429.
- (12) Babonneau, F.; Camus, L.; Steunou, N.; Rámila, A.; Vallet-Regí, M. Encapsulation of Ibuprofen in Mesoporous Silica: Solid State NMR Characterization. *Mater. Res. Soc. Symp. Proc.* **2003**, *775*, 77–82.
- (13) Babonneau, F.; Yeung, L.; Steunou, N.; Gervais, C.; Rámila, A.; Vallet-Regí, M. Solid State NMR Characterisation of Encapsulated Molecules in Mesoporous Silica. *J. Sol–Gel Sci. Technol.* **2004**, *31*, 219–223.
- (14) Azais, T.; Hartmeyer, G.; Quignard, S.; Laurent, G.; Tourné-Péteilh, C.; Devoisselle, J.-M.; Babonneau, F. Solid-State NMR Characterization of Drug-Model Molecules Encapsulated in MCM-41 Silica. *Pure Appl. Chem.* **2009**, *81*, 1345–1355.
- (15) Dudognon, E.; Danède, F.; Descamps, M.; Correia, N. T. Evidence for a New Crystalline Phase of Racemic Ibuprofen. *Pharm. Res.* **2008**, *25*, 2853–2858.
- (16) Charnay, C.; Bégu, S.; Tourné-Péteilh, C.; Nicole, L.; Lerner, D. A.; Devoisselle, J. M. Inclusion of Ibuprofen in Mesoporous Templated Silica: Drug Loading and Release Property. *Eur. J. Pharm. Biopharm.* **2004**, *57*, 533–540.
- (17) Ruiz-Hitzky, E.; Ariga, K.; Lvov, Y. M., Eds. Bio–Inorganic Hybrid Nanomaterials: Strategies, Syntheses. *Characterization and Applications*; Wiley-VCH: New York, 2008.
- (18) Salonen, J.; Kaukonen, A. M.; Hirvonen, J.; Lehto, V. P. Mesoporous Silicon in Drug Delivery Applications. *J. Pharm. Sci.* **2008**, *97*, 632–653.
- (19) McConnell, J. F. The 2-(4-Isobutylphenyl) Propionic Acid. Ibuprofen or Prufen. *Cryst. Struct. Commun.* **1974**, *3*, 73–75.
- (20) Shankland, N.; Wilson, C. C.; Florence, A. J.; Cox, P. C. Refinement of Ibuprofen at 100K by Single-Crystal Pulsed Neutron Diffraction. *Acta Crystallogr., Sect. C* **1997**, *53*, 951–954.
- (21) Brás, A. R.; Noronha, J. P.; Antunes, A. M. M.; Cardoso, M. M.; Schönhals, A.; Affouard, F.; Dionísio, M.; Correia, N. T. Molecular Motions in Amorphous Ibuprofen as Studied by Broadband Dielectric Spectroscopy. *J. Phys. Chem. B* **2008**, *112*, 11087–11099.
- (22) Derollez, P.; Dudognon, E.; Affouard, F.; Danède, F.; Correia, N. T.; Descamps, M. Ab Initio Structure Determination of Phase II of Racemic Ibuprofen by X-ray Powder Diffraction. *Acta Crystallogr., Sect. B* **2010**, *66*, 76–80.
- (23) Brás, A. R.; Frunza, S.; Guerreiro, L.; Fonseca, I. M.; Corma, A.; Frunza, L.; Dionísio, M.; Schönhals, A. Molecular Mobility of Nematic E7 Confined to Molecular Sieves with a Low Filling Degree. *J. Chem. Phys.* **2010**, *132*, 224508/1–224508/12.
- (24) Silverstein, R. M.; Bassler, G. C.; Morrill, T. C. *Spectrometric Identification of Organic Compounds*, 5th ed.; John Wiley & Sons: New York, 1991.
- (25) Schönhals, A.; Kremer, F. Analysis of Dielectric Spectra. In *Broadband Dielectric Spectroscopy*; Kremer, F., Schönhals, A., Eds.; Springer Verlag: Berlin, Germany, 2003; Chapter 3.
- (26) Boersma, A.; Van Turnhout, J.; Wübbenhorst, M. Dielectric Characterization of a Thermotropic Liquid Crystalline Copolyester-

amide: 1. Relaxation Peak Assignment. *Macromolecules* **1998**, *31*, 7453–7460.

(27) Schröter, K.; Unger, R.; Reissig, S.; Garwe, F.; Kahle, S.; Beiner, M.; Donth, E. Dielectric Spectroscopy in the $\alpha\beta$ Splitting Region of Glass Transition in Poly(ethyl methacrylate) and Poly(*n*-butyl methacrylate): Different Evaluation Methods and Experimental Conditions. *Macromolecules* **1998**, *31*, 8966–8972.

(28) Vogel, H. The Temperature Dependence Law of the Viscosity of Fluids. *Phys. Z.* **1921**, *22*, 645–646.

(29) Fulcher, G. S. Analysis of Recent Measurements of the Viscosity of Glasses. *J. Am. Ceram. Soc.* **1925**, *8*, 339–355.

(30) Tammann, G.; Hesse, W. The Dependency of Viscosity on Temperature in Hypothermic Liquids. *Z. Anorg. Allg. Chem.* **1926**, *156*, 245–257.

(31) Smith, W.; Forester, T. R. DL_POLY_2.0: A General-Purpose Parallel Molecular Dynamics Simulation Package. *J. Mol. Graphics* **1986**, *14*, 136–141.

(32) Jorgensen, W. L.; Maxwell, D.; Tirado-Rives, J. Development and Testing of the OPLS All-Atom Force Field on Conformational Energetics and Properties of Organic Liquids. *J. Am. Chem. Soc.* **1996**, *118*, 11225–11236.

(33) Ryckaert, J. P.; Ciccotti, G.; Berendsen, H. J. C. Numerical Integration of the Cartesian Equations of Motion of a System with Constraints: Molecular Dynamics of *n*-alkanes. *J. Comput. Phys.* **1977**, *23*, 327–341.

(34) Hockney, R. W. The Potential Calculation and Some Applications. *Methods Comput. Phys.* **1970**, *9*, 136–211.

(35) Berendsen, H. J. C.; Postma, J. P. M.; van Gunsteren, W. F.; DiNola, A.; Haak, J. R. J. Molecular Dynamics with Coupling to an External Bath. *Chem. Phys.* **1984**, *81*, 3684–3690.

(36) Busselez, R.; Lefort, R.; Ji, Q.; Affouard, F.; Morineau, D. Molecular Dynamics Simulation of Nanoconfined Glycerol. *Phys. Chem. Chem. Phys.* **2009**, *11*, 11127–11133.

(37) Vink, R. L. C.; Barkema, G. T. Large Well-Relaxed Models of Vitreous Silica, Coordination Numbers, and Entropy. *Phys. Rev. B* **2003**, *67*, 245201.

(38) Puibasset, J.; Pellenq, R. J. -M. Grand Canonical Monte Carlo Simulation Study of Water Structure on Hydrophilic Mesoporous and Plane Silica Substrates. *J. Chem. Phys.* **2003**, *119*, 9226–9232.

(39) Guégan, R.; Morineau, D.; Alba-Simionesco, C. Interfacial Structure of an H-Bonding Liquid Confined into Silica Nanopore with Surface Silanols. *Chem. Phys.* **2005**, *317*, 236–244.

(40) Kresge, C. T.; Leonowicz, M. E.; Roth, W. J.; Vartuli, J. C.; Beck, J. S. Ordered Mesoporous Molecular Sieves Synthesized by a Liquid-Crystal Template Mechanism. *Nature* **1992**, *359*, 710–712.

(41) Tanis, I.; Karatasos, K. Association of a Weakly Acidic Anti-Inflammatory Drug (Ibuprofen) with a Poly(Amidoamine) Dendrimer as Studied by Molecular Dynamics Simulations. *J. Phys. Chem. B* **2009**, *113*, 10984–10993.

(42) Berendsen, H. J. C.; Postma, J. P. M.; van Gunsteren, W. F.; DiNola, A.; Haak, J. R. Molecular Dynamics with Coupling to an External Bath. *J. Chem. Phys.* **1984**, *81*, 3684–3690.

(43) Arndt, M.; Stannarius, R.; Groothues, H.; Hempel, E.; Kremer, F. Length Scale of Cooperativity in the Dynamic Glass Transition. *Phys. Rev. Lett.* **1997**, *79*, 2077–2080.

(44) Frunza, L.; Frunza, S.; Kosslick, H.; Schönhals, A. Phase Behavior and Molecular Mobility of *n*-Octylcyanobiphenyl Confined to Molecular Sieves: Dependence on the Pore Size. *Phys. Rev. E* **2008**, *78*, 051701.

(45) Schüller, J.; Mel'nichenko, Y. B.; Richert, R.; Fischer, E. W. Dielectric Studies of the Glass Transition in Porous Media. *Phys. Rev. Lett.* **1994**, *73*, 2224–2227.

(46) Ngai, K. L. *Relaxation and Diffusion in Complex Systems*; Springer: New York, 2011; Chapter 2 and references therein.

(47) Johari, G. P.; Goldstein, M. Viscous Liquids and the Glass Transition. II. Secondary Relaxations in Glasses of Rigid Molecules. *J. Chem. Phys.* **1970**, *53*, 2372–2388.

(48) Johari, G. P.; Goldstein, M. Viscous Liquids and the Glass Transition. III. Secondary Relaxations in Aliphatic Alcohols and Other Nonrigid Molecules. *J. Chem. Phys.* **1971**, *55*, 4245–4252.

(49) Ngai, K. L. An Extended Coupling Model Description of the Evolution of Dynamics with Time in Supercooled Liquids and Ionic Conductors. *J. Phys.: Condens. Matter* **2003**, *15*, S1107–S1125.

(50) Ngai, K. L.; Paluch, M. Classification of Secondary Relaxation in Glass-Formers Based on Dynamic Properties. *J. Chem. Phys.* **2004**, *120*, 857–873.

(51) Kohlrausch, R. Nachtrag über die Elastische Nachwirkung beim Cocon und Glasfaden, und die Hygroskopische Eigenschaft des Ersteren. *Poggendorff's Ann. Phys. III* **1847**, *12*, 393–399.

(52) Kohlrausch, R. Theorie des Electricischen Rückstandes in der Leidener Flasche. *Poggendorff's Ann. Phys. IV* **1854**, *1*, 79–86.

(53) Williams, G.; Watts, D. C. Non-Symmetrical Dielectric Relaxation Behaviour Arising from a Simple Empirical Decay Function. *Trans. Faraday Soc.* **1970**, *66*, 80–85.

(54) Alegria, A.; Guerrica-Echevarria, E.; Goitandia, L.; Telleria, I.; Colmenero, J. α -Relaxation in the Glass Transition Range of Amorphous Polymers. 1. Temperature Behavior Across the Glass Transition. *Macromolecules* **1995**, *28*, 1516–1527.

(55) Alvarez, F.; Alegria, A.; Colmenero, J. Relationship Between the Time-Domain Kohlrausch–Williams–Watts and Frequency-Domain Havriliak–Negami Relaxation Functions. *Phys. Rev. B* **1991**, *44*, 7306–7312.

(56) Kudlik, A.; Tschirwitz, C.; Blochowicz, T.; Benkhof, S.; Rössler, E. Slow Secondary Relaxation in Simple Glass Formers. *J. Non-Cryst. Solids* **1998**, *235–237*, 406–411.

(57) Ngai, K. L.; Capaccioli, S. Relation between the Activation Energy of the Johari–Goldstein β Relaxation and T_g of Glass Formers. *Phys. Rev. E* **2004**, *69*, 031501.

(58) Hartmann, L.; Kremer, F.; Pouret, P.; Léger, L. Molecular Dynamics in Grafted Layers of Poly(dimethylsiloxane). *J. Chem. Phys.* **2003**, *118*, 6052–6058.

(59) Schönhals, A.; Goering, H.; Schick, Ch.; Frick, B.; Zorn, R. Polymers in Nanoconfinement: What Can Be Learned from Relaxation and Scattering Experiments? *J. Non-Cryst. Solids* **2005**, *351*, 2668–2677.

(60) Ngai, K. L. Predicting the Changes of Relaxation Dynamics with Various Modifications of the Chemical and Physical Structures of Glass-Formers. *J. Non-Cryst. Solids* **2007**, *353*, 4237–4245.

(61) Böhmer, R.; Ngai, K. L.; Angell, C. A.; Plazek, D. J. Nonexponential Relaxations in Strong and Fragile Glass Formers. *J. Chem. Phys.* **1993**, *99*, 4201–4209.

(62) Moynihan, C. T.; Macebo, P. B.; Montrose, C. J.; Gupta, P. K.; DeBolt, M. A.; Dill, J. F.; Dom, B. E.; Drake, P. W.; Esteal, A. J.; Elterman, P. B.; et al. Structural Relaxation in Vitreous Materials. *Ann. N.Y. Acad. Sci.* **1976**, *279*, 15–35.

(63) León, C.; Ngai, K. L. Rapidity of the Change of the Kohlrausch Exponent of the α -Relaxation of Glass-Forming Liquids at T_B or T_β and Consequences. *J. Phys. Chem. B* **1999**, *103*, 4045–4051.

(64) Casalini, R.; Ngai, K. L.; Roland, C. M. Connection Between the High-Frequency Crossover of the Temperature Dependence of the Relaxation Time and the Change of Intermolecular Coupling in Glass-Forming Liquids. *Phys. Rev. B* **2003**, *68*, 014201/1–014201/5.

(65) Merino, E. G.; Neves, P. D.; Fonseca, I. M.; Danède, F.; Idrissi, A.; Dias, C. J.; Dionísio, M.; Correia, N. T. Detection of Two Glass Transitions on Triton X-100 under Confinement. *J. Phys. Chem. C* **2013**, *117*, 21516–21528.

(66) Böttcher, C. J. F. *Theory of Dielectric Polarization*; 2nd ed., Elsevier: Amsterdam, The Netherlands, 1973; Vol. I.

(67) Böttcher, C. J. F.; Bordewijk, P. *Theory of Dielectric Polarization*; Elsevier: Amsterdam, The Netherlands, 1978; Vol. 2.

(68) Schönhals, A.; Kremer, F. Theory of Dielectric Relaxation. In *Broadband Dielectric Spectroscopy*; Kremer, F., Schönhals, A., Eds.; Springer Verlag: Berlin, Germany, 2003; Chapter 1.

(69) Schönhals, A. Molecular Dynamics in Polymer Model Systems. In *Broadband Dielectric Spectroscopy*; Kremer, F., Schönhals, A., Eds.; Springer Verlag: Berlin, Germany, 2003; Chapter 7.

(70) Affouard, F.; Correia, N. T. Debye Process in Ibuprofen Glass-Forming Liquid: Insights from Molecular Dynamics Simulation. *J. Phys. Chem. B* **2010**, *114*, 11397–11402.